WEAR-TYPE RAIL CORRUGATION PREDICTION: PASSAGE TIME DELAY EFFECTS

Meehan, P.A.* and Daniel, W.J.T.

CRC for Railway Engineering and Technologies, Mechanical Engineering, University of Queensland, Australia

Abstract

The growth behaviour of the vibrational wear phenomenon known as rail corrugation is investigated using analytical and numerical models. A feedback model for wear-type rail corrugation that includes a wheel pass time delay is investigated with an aim to determine what effects the time between successive wheel passages has on the growth of the amplitude of corrugations. The feedback model is simplified to encapsulate the most critical interactions occurring between the wheel/rail structural dynamics, rolling contact mechanics and rail wear. A stability analysis on the system yields the growth of wear-type rail corrugations over multiple wheelset passages as a function of the passage time delay magnitude. Based on these results, numerical and analytical investigations are performed to identify conditions under which the passage time delay has a significant effect on the growth of corrugations.

Nomenclature

C_ξ	Sensitivity of creep to contact force variations
G_{r_i}	Modal growth rate parameter
k_0	Wear coefficient
k_c	Contact stiffness
K_b	Sensitivity of the steady state response of wheel/rail relative displacement to a step change in input longitudinal profile
K_{c_i}	Modal sensitivity of the steady state response of wheel/rail relative displacement to a step change in input longitudinal profile
Ł	Laplace transform operator
m_i , ω_i , ζ_i	Modal mass, natural frequency, damping
n	Number of modes
N	Wheelset pass number
p_i	Element of the modal matrix
P_0	Nominal contact force
S	Nondimensionalised Laplace transform complex variable
t , τ	Dimensional, nondimensional time
Δt	Wheel pass time delay
V	Vehicle speed
x	Distance along rail track
y_i , Y_i	Time, Laplace domain modal displacement of vertical wheelset rail dynamics
y_r	Vertical displacement of rail
y_w	Vertical displacement of the wheelset
z_{in} , Z_{in} / z_{out} , Z_{out}	Time, Laplace domain rail longitudinal profile variation, from steady state wear, entering/exiting the rolling contact region
α , β_i	System parameter
ω_d	Nondimensional damped oscillation frequency
Δz_0	Nominal steady state change in profile per wheelset pass

Subscript

i	Modal parameter (mode i)

Introduction

Rail corrugation is a rolling contact vibration phenomenon characterised by the development of highly undesirable, irregular, wear patterns on railway track. These corrugations induce vibrations as vehicles pass over them, causing excessive noise, restricting running speeds and in some cases causing serious track defects. The phenomenon has remained persistent and grown in prevalency, worldwide, in its multiple forms over many decades [1]. Wear-type rail corrugations include those classified as "rutting" and "roaring rails"[1], characterised by both long (100-400mm) and short pitch wavelengths (25-80mm). The resultant railway noise due to short pitch wavelengths is in the range of 200-1500Hz and is particularly undesirable in populated areas. At present the only reliable cure for wear-type rail corrugation is removal by grinding, which costs the railway industry substantially in maintenance expenditure per annum [2]. These costs appear to be increasing in line with the significant increase in usage, development and speed of railways throughout the world.

Much research has been focused on prediction and prevention of rail corrugation recently. Recent research in Germany[3], Sweden[4] and Japan[5] amongst others has resulted in the development of integrated simulation programs incorporating complex finite element models for the dynamics of the track and discrete element models for the rolling contact mechanics. Recently Wu and Thompson [6] have numerically investigated the effect of multiple wheel/track passes using a frequency domain model. To provide fundamental insight, a number of efforts have also been directed towards obtaining analytical predictions of wear-type rail corrugation [2,7,8]. Muller [2] and Nielsen [8] have investigated a non-linear contact mechanics filter to explain reports of the independence of wavelength with speed for shorter pitch corrugations. However the investigations neglected the effect of wheel/rail structural

dynamic components on growth. Bhaskar et al [7] and Muller [2] investigated the stability of the interaction between the structural dynamics and contact mechanics over one wheelset passage. Recently, Meehan et al [9] extended this research, providing an analytical prediction of the growth of wear type rail corrugation over multiple wheelset passes. However the effect of dynamic interactions between multiple wheel passages was not fully investigated for short passage delays.

In the present analysis, the growth behaviour of wear-type rail corrugation is investigated to determine specifically what effects the time delay between successive wheel passages has on the growth of the amplitude of corrugations. The feedback model developed in [9] is utilised which encapsulates the most critical interactions occurring between the wheel/rail structural dynamics, rolling contact mechanics and rail wear. Using this model, numerical and analytical investigations are performed to identify conditions under which the passage time delay has a significant effect on the growth of corrugations. In particular, a stability analysis on the complete system is extended to determine the growth of wear-type rail corrugations over multiple wheelset passages. This is investigated further using numerical models. The analysis is also pertinent to the dynamic wear behaviour of two-disc test rigs.

Analysis of Rail Corrugation over multiple wheel passages

The system diagram shown in Figure 1 describes the wear-type rail corrugation development feedback mechanism. Meehan et al [9] provides a detailed description and derivation of this model.

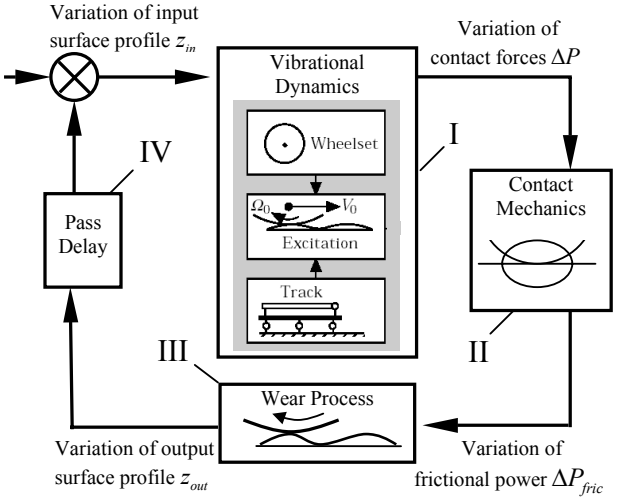

Figure 1. Feedback model for wear-type rail corrugation

The wheelset track vibrational dynamics, I, may be described by a decoupled equation of motion for each mode, in the real analytical form,

$$\ddot{y}_i + 2\zeta_i\omega_i\dot{y}_i + \omega_i^2 y_i = k_c z_{in}(p_i - 1)/m_i \ . \qquad (1)$$

The coordinate transform for the modal displacements, y_i, are given by,

$$y_w = \sum_{i=1}^{n} p_i y_i \ , \ y_r = \sum_{i=1}^{n} y_i \ . \qquad (2)$$

The equations governing the contact mechanics, II, and wear process, III, can be combined and solved for each mode to give,

$$\left(z_{out_i} - z_{in_i}\right)\Big/\Delta z_0 = C_\xi k_c \left(y_i\left(1-p_i\right) + z_{in_i}\right)\Big/P_0 \ . \qquad (3)$$

For multiple wheel passages, rail profile variation entering the rolling contact region of the wheelset, $z_{in}(x)$, is the same rail profile variation exiting from the previous wheelset pass, $z_{out}(x)$. Therefore, assuming a time interval between wheelset passes, Δt, the profile wear of successive passes of wheelsets is represented by the time delay relationship,

$$z_{in}(t) = z_{out}(t - \Delta t) \qquad (4)$$

Using the Laplace transform denoted as,

$$Ł\left\{f(\omega_i t)\right\} = F(S) \ , \qquad (5)$$

equations (1) and (3) may be solved to obtain,

$$Z_{out_i}/Z_{in_i} = 1 + K_b\left[1 - K_{c_i}\Big/\left(S^2 + 2\zeta_i S + 1\right)\right], \qquad (6)$$

where,

$$K_b = C_\xi k_c \Delta z_0 / P_0 \ , \ K_{c_i} = k_c(1-p_i)^2/m_i\omega_i^2 \ . \qquad (7)$$

Equation (6) represents the dynamic behaviour of the system over one wheelset passage. K_b represents the sensitivity of wear variations to wheel/rail contact deflection variations. Similarly, K_{c_i} may be shown to represent the modal sensitivity of the wheel/rail relative displacement to a change in input longitudinal profile. For realistic railway parameters, K_b, K_{c_i} and ζ_i are always positive valued. Under these assumptions, it may be easily shown, using renowned stability analysis techniques, that the second order system, (6), is always stable, in line with [2] and [7].

To investigate the behaviour over multiple wheelset passages, the passage time delay equation (4) is also transformed into the Laplace form,

$$Z_{in_i}/Z_{out_i} = e^{-S\omega_i\Delta t} \ . \qquad (8)$$

Equations (6) and (8) describe a single input – single output feedback system that may also be represented by a block diagram equivalent to *figure 1* [9]. The stability behaviour of the system may be determined analytically from the characteristic equation for the complete system. The characteristic equation may be obtained by solving equations (6) and (8) as,

$$1 - (1+K_b)\left(1 - \frac{\beta_i}{S^2 + 2\zeta S + 1}\right)e^{-S\omega_i\Delta t} = 0 \ , \qquad (9)$$

where

$$\beta_i = \frac{K_b K_{ci}}{1+K_b}. \quad (10)$$

The stability behaviour of the system is determined by the dominant real part of the system closed loop poles which are the roots to the characteristic equation (9), described by the nondimensional expression,

$$S = \sigma + \omega_d j, \quad (11)$$

where j denotes the imaginary component. The characteristic equation (9) may be considered to define both magnitude and phase conditions due to the complex nature of the roots, S. The non-trivial solutions to these conditions are developed under the realistic assumptions [9],

$$0 < K_b << \zeta_i << 1,$$
$$0 < \beta_i << \zeta_i << 1,$$
$$|\sigma| << \zeta_i << 1,$$

and are summarised in the following.

Phase condition

The phase condition of (9) provides the solution for the imaginary component of the closed loop poles as,

$$\omega_d = \pm \frac{2\pi}{\omega_i \Delta t} n, \quad n = 0,1,2 \ldots \quad (12)$$

Equation (12) defines an infinite number of closed loop poles at equally spaced intervals along the imaginary axis of the root locus. Each solution to (12) represents a frequency (or corrugation wavelength) that will be present in the response of the system. The infinite number of roots (or order) of the system arises due to the nonlinear passage time delay term. The effect of the magnitude of the wheel pass time delay Δt on the system behaviour via equation (12) is investigated and discussed subsequently.

Magnitude condition

Solution for the magnitude condition of (9) yields an expression for the real part of the system poles,

$$\sigma \approx \frac{1}{\omega_i \Delta t} \ln\left[\left(1+K_b\right)\left(1 + \frac{\beta_i\left(\omega_d{}^2 - 1\right)}{\left(1-\omega_d{}^2\right)^2 + \left(2\zeta_i \omega_d\right)^2} \right) \right]. \quad (13)$$

Equations (11)-(13) define the analytical solution for all the closed loop system poles. The stability of the system and hence the growth of corrugations may be determined from equation (13). In particular, the growth rate of instability for mode i, defined by parameter G_{r_i} can be expressed as the magnitude of the transfer function (see [9]),

$$\left| Z_{out_i} / Z_{in_i} \right| = 1 + G_{r_i} = e^{\sigma \omega_i \Delta t}. \quad (14)$$

The dominant pole (or mode) magnitude is determined by finding the critical value for the imaginary component, ω_d, for which the maximum value for σ occurs. This is given by,

$$\omega_d{}^2 = 1 + 2\zeta_i. \quad (15)$$

This maximum value for growth is typically not realised exactly as the system phase condition described by (12) must be satisfied. If the parameter $\omega_i \Delta t$ is typically very large, the discretisation of ω_d, defined by (12), is small enough such that there will always be a pole that approximately satisfies (15) to sufficient accuracy. In this case, each wheelset passage occurs after the dynamic effects of the previous wheelset have settled down to a negligible level. This assumption has been made in previous research ie [3,4,7,8] and may be used to simplify the growth rate to the form,

$$G_{r_i} \approx K_b \left(1 + K_{c_i} / 4\zeta_i \left(1+\zeta_i\right)\right), \quad (16)$$

assuming a small k_0. For the consideration of adjacent wheels on a bogie travelling at considerably high speeds, it is expected that the approximation, (16), will not be as accurate as for low speeds. Greater accuracy will be obtained if the value for ω_d that satisfies (12) and is closest to satisfying (15) is used. In this case, the magnitude of the passage time delay may or may not have a substantial effect on the growth rate of corrugations due to the phase between the previous and present pass dynamics. This is investigated quantitatively in the following sections using simplified and finite element, time domain models.

Two Mode Model Wear Predictions

The analytical solutions for rail profile wear (12)-(16) were compared with that obtained via numerical integration based on a discrete system model described in [9]. The vibrational dynamics is represented by two vertical vibration modes and incorporated with Hertzian rolling contact mechanics and frictional wear models for rail longitudinal wear. Analytical and numerical simulations of wear resulting from an initial bump on a flat profile over multiple wheel passages were obtained for infinite and short passage time delays. For comparison, both the analytical and numerical results use the parameters of Table 1 with $k_0 = 10^{-9}\left[kg/Nm\right]$. These parameters are the scaled railway conditions of [9] for a two-disk test-rig (contact stress is equivalent). A numerical step size of 10^{-4}m was chosen to achieve adequate convergence of solutions.

Table 1. Railway parameters for simulation

Train speed [m/s]	34.7	Track length/pass [m]	30
Wheel mass [kg]	49.73	Rail density [kg/m]	7800
Wheel radii -long. [m]	0.085	Rail radii -long. [m]	0.213
- trans. [m]	0.04	-trans.[m]	0.05
Wheel load [N]	400	Coef. of friction	0.4
Young's modulus [N/m^2]	2.1×10^{11}	Primary rail damping	0.01
Poisson's ratio	0.3	Bump length [mm]	0.012
Shear modulus [Pa]	7.7×10^{10}	Bump height [m]	10^{-7}
Rail disc mass [kg]	32.06	Contact damping	0.0021

An example of the results is shown in Fig. 2. In particular, the rail wear, $z_{out_i N}$, over 50,000 passages for short (0.865s) and infinite pass delays are plotted versus rail track position variable, *x*, assuming constant vehicle velocity *V*=*xt*.

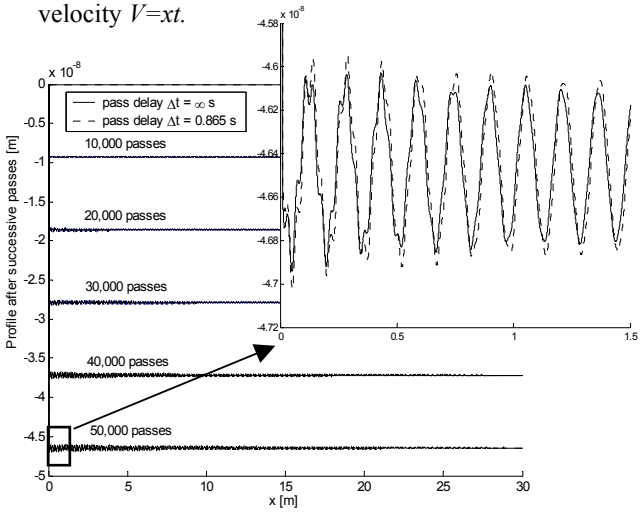

Figure 2. Corrugation growth over 50,000 passes.

The growth in amplitude of the dominant frequency wear is plotted in Fig. 3 using an FFT analysis and the analytical results of (12)-(16). The wear is expressed as a profile ratio, which is defined as $z_{out_i N} / z_{in_i 1}$ for the lower frequency mode of wear. Table 2 summarizes the results for growth rate for both the dominant modes.

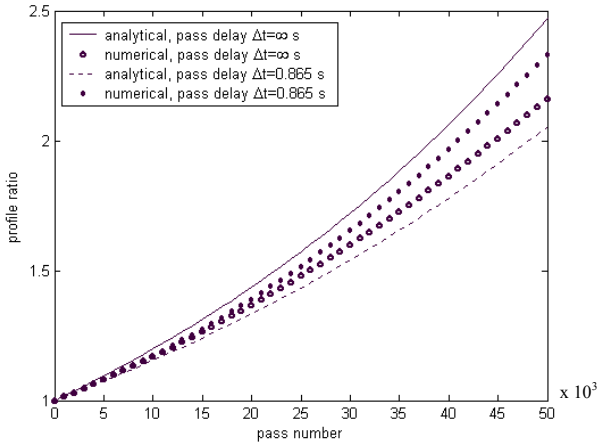

Figure 3. Corrugation amplitude growth of 223 Hz mode.

Table 2. Growth rate comparisons

	G_r of low frequency (223 Hz)	G_r of high frequency (954 Hz)
Δt =0.865s Numerical	0.0171	0.0005
Δt =0.865s Analytical	0.0144	0.0005
Δt =∞ s Numerical	0.0156	0.0005
Δt =∞ s Analytical	0.0183	0.0005

Figures 2 and 3 predict that the passage time delay has an effect on the growth of corrugations for the conditions chosen but results are fairly close to the analytical prediction for infinite time delay, (16). It was of interest to investigate the effect of small changes in time delay (or speed) on these results. As such, the growth rate of corrugations was determined for the same conditions of Table 1 for a range of vehicle speeds, as shown in Fig.4, for the low frequency mode.

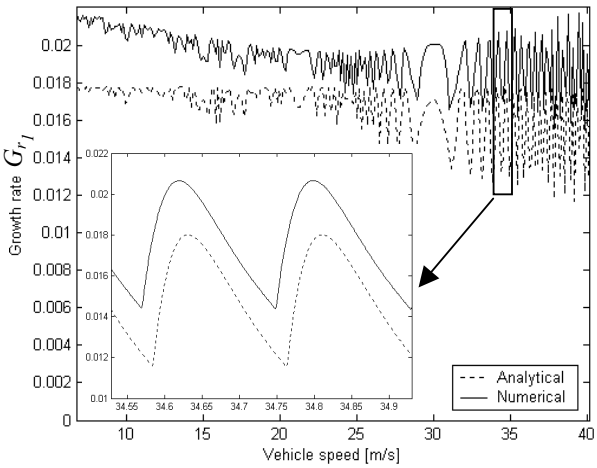

Figure 4. Corrugation growth rate versus time delay. 50,000 passes. Track length/pass = 30m.

Figure 4 shows that the growth rate can be very sensitive to vehicle speed (or passage time delay). In particular, as the time delay gets smaller the growth rate becomes more sensitive to its value. This is evident in the numerical results as well. By inspection of eqs (12) and (13) it may be seen that this sensitivity is an artefact of the phase relationship discussed previously. In particular, the blowup section of Fig. 4 indicates that the growth rate variation is periodic with a period equal to $\omega_i \Delta t \approx 2\pi$. This is consistent with the discretisation of the closed loop poles defined by equation (18). The maximum growth rate at any speed occurs when,

$$\omega_i \Delta t = n \frac{2\pi}{\sqrt{1+2\zeta_i}}, \quad n = 0,1,2 \ldots \qquad (17)$$

which is in accordance with eqs (12) and (15). The comparison between analytical and numerical results is good with the small offset likely due to numerical errors associated with the FFT method and/or nonlinearities.

Corrugation growth was also investigated under conditions of larger variations from nominal conditions. Figure 5 illustrates such a case for a shorter track length

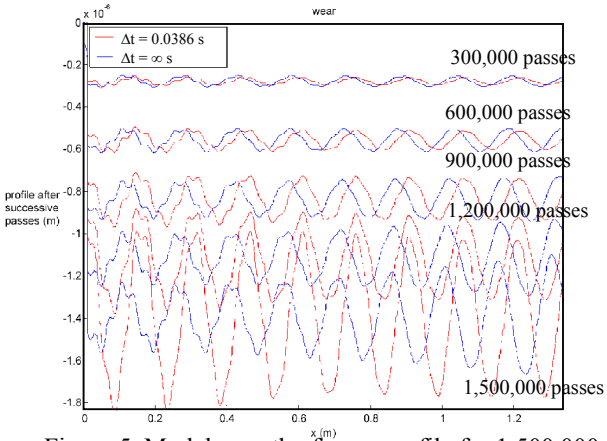

Figure 5. Modal growth of wear profile for 1,500,000 passes. Track length/pass = 1.34m.

per pass over 1.5 million passes. Under these conditions, the short time delay growth greatly exceeds the infinite case, particularly once the wavelength ratio becomes an integer. In particular, the wavelength of corrugations for the short time delay case becomes fixed at an integer value of 9 in accordance with the predictions of (12). In contrast, infinite time delay case shows a wavelength that is varying with the number of passages most likely due to the nonlinearities associated with the large contact force variations. At the final pass, the variation in contact force is ±80% of the nominal condition indicating highly nonlinear conditions have been reached. Although this case may not be of common practical concern, it would be of interest to determine the exact nature of the nonlinear behaviour involved. It is noted that for linear conditions (small number of passes) the corrugation growth was found to be similar in both cases.

For a more detailed numerical investigation, accounting for all the modes of vibration, a finite element model was developed as described subsequently.

Finite Element Wear Predictions

Rail wear due to two 350kg wheels, 2.4m apart, repeatedly traversing a track has been studied with a conventional finite element rail model. The model is benchmarked and documented in [9] and the same parameters are used presently, except for the sleeper spacing, which is set at 0.685m to correspond to Queensland practice. This spacing corresponds to 3.5 sleepers over the wheelbase. The rail consists of 5 Timoshenko beam elements per sleeper. The sleepers are lumped masses, as are the wheels. Ties and ballast are modelled with discrete springs and dampers. The equations for vertical motion are derived from equilibrium under gravity, in order to remove any excitation due to multiples of sleeper-passing frequency. A contact smoothing algorithm is used to avoid any artifacts in the spectrum from the wheels crossing from one rail element to the next. The profile of the track is computed from estimated frictional power, filtering the highest frequencies from the rail profile, to allow for the finite size of the wheel-rail contact zone. The wheel is first moved along the rail in a series of direct time integration runs with the train speed set to 35 m s^{-1} giving a short pass delay, Δt, of 0.0686 s. The peak growth of corrugation in response to an initial random profile is found to be at 791.4 Hz. The spectrum of corrugation obtained is shown in Figure 6. Response around each natural frequency is discretised at intervals of wheel-passing frequency ($1/\Delta t$) in accordance with (12), a fact not revealed in previous studies. The damped natural frequencies and modes of vibration of the track model with two wheels on it have been found from a complex eigenvalue analysis in the Abaqus package. This reveals that the mode responding near 791.4 Hz corresponds to 3 semi-wavelengths of bending of the rail between the wheels.

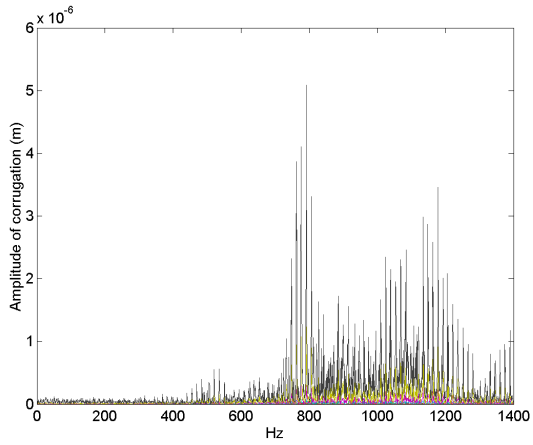

Figure 6: Spectrum of rail wear at wheel spacing 2.4m, speed 35 m/s

This agrees with the observation of Igeland [10] that peak corrugation responses occur in modes with integer multiples of a semi-wavelength between the wheels. The peaks near 1200 Hz correspond to about 4 semi-wavelengths between the wheels. In order to tune the excitation of the 791.4 Hz mode, the speed of the train is adjusted slightly to 35.1725 m s^{-1}, making this resonance 54 times wheel-passing frequency. This tuning of the excitation increases the growth of corrugation at this resonant frequency by 33%.

If the wheel spacing is changed to 2.74m, making it match 4 sleeper spacings, then a peak response at speeds close to 31 m s^{-1} occurs largely in wheel/rail modes around 1080 Hz. However, very slight changes in train speed greatly influence the response in these modes. The spectrum of corrugation resembles that shown in Figure 7 and is again discretized at intervals of wheel-passing frequency – 11 Hz.

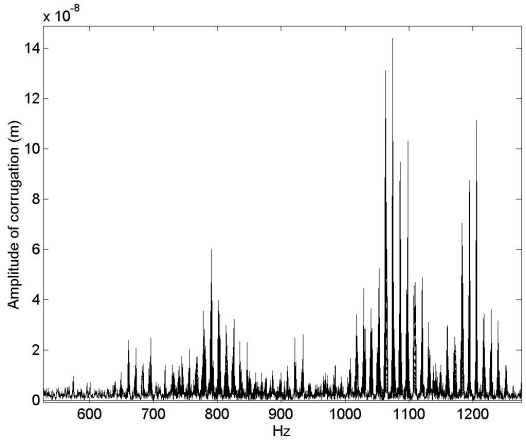

Figure 7: Spectrum of rail wear at wheel spacing 2.74m, train speed of 31.09 m/s.

Which of the 4 peaks seen in the spectrum near 1080 Hz grows the most (1064 Hz, 1075 Hz, 1086 Hz or 1097 Hz) changes with small speed changes.

Figure 8 shows the changes in the peak growth of corrugation after 15 million simulated passes and the

vibration frequency associated with the corrugation in each case.

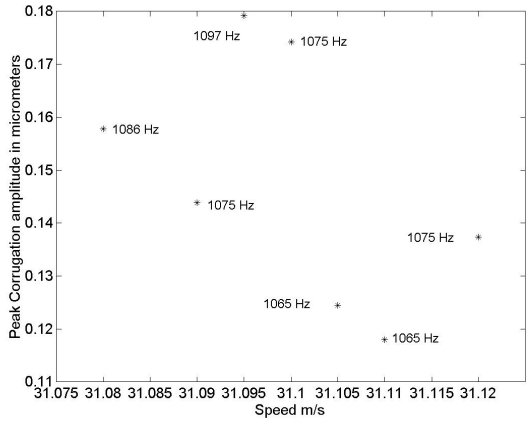

Figure 8. Effect of speed on corrugation growth near 31.1m/s

Each data point is from a different two-wheel simulation. The simulations change the speed of the train by only ± 0.02 m s^{-1} about 31.1 m s^{-1}. Hence while the overall envelope of corrugation growth versus frequency, is predictable, the detail of growth at a particular frequency is critically speed dependent. These results are consistent with analytical and numerical predictions shown in the previous section (eg fig. 4), although the presence and interaction of multiple modes has added complexity.

Conclusions

Analytical predictions have been developed for the growth of wear-type rail corrugation showing the effect of the time delay between successive multiple wheel passages. These predictions are based on a simplified feedback model that encapsulates the most critical interactions occurring between the wheel/rail structural dynamics, rolling contact mechanics and rail wear. Numerical and analytical investigations have identified conditions under which the passage time delay has a significant effect on the growth of corrugations. The results indicate that the phase relationship between the wheel/track vibrations and wheel passages is a critical factor determining the magnitude of the effects on growth when the passage time delay is small. In particular the growth is shown to very sensitive to the time delay when it is small, however this variation is well predicted by the analytical solution.

The model of two wheels on finite element rails shows the sensitivity of growth to a short time-delay, as a discretization of the spectrum of corrugation. The growth at higher frequencies is found to be very sensitive to this parameter, the peak response switching by one or more multiples of wheel-passing frequency with a very small change of train speed.

The analytical model provides a useful means by which to predict this sensitivity. A limitation of the analytical solution is that it is restricted to the initiation of corrugation growth when the amplitude is small such that the linear assumptions are valid. For larger amplitude growth numerical simulation indicates that corrugation growth exceeds the analytical predictions due to nonlinearities. This could be investigated more thoroughly. Future research on the influence of sleepers and initial rail irregularity on growth would also be prudent as well as validation via experimental results.

Acknowledgements

The authors are grateful for the support of the Rail CRC, Queensland Rail, Rail Infrastructure Corporation and the Australian Rail Track Corporation and the assistance of Mr F. Fraysse and Mr G. Lasserre with simulations.

References

[1] S. L. Grassie, and J. Kalousek, Rail corrugation: characteristics, causes and treatments, Proceedings of The Institution of Mechanical Engineers, Part F 207 (1993) 57-68.

[2] S. Muller, A linear wheel-rail model to investigate stability and corrugation on straight track, Wear 249 (2001) 1117-1127.

[3] K. Hempelmann and K. Knothe, An extended linear model for the prediction of short pitch corrugation, Wear 191 (1996) 161-169.

[4] A. Igeland, and H. Ilias, Rail Head Corrugation Growth Predictions Based On Non-Linear High Frequency Vehicle/Track Interaction, Wear 213 (1997) 90-97.

[5] A. Matsumoto, Y. Sato, et al. Study on the Formation Mechanism of Rail Corrugation on Curved Track. Vehicle System Dynamics 25 (1996) 450-465.

[6] T. W. Wu and D. J. Thompson, An Investigation into rail corrugation due to microslip under multiple wheel/rail interactions, Proceedings of the 6th International Conference on Contact Mechanics and Wear of Rail/Wheel Systems(CM2003) in Gothenburg, Sweden, June 10-13, (2003) 59-67

[7] A. Bhaskar, K. L. Johnson, G. D. Wood, and J. Woodhouse, Wheel –rail dynamics with closely conformal contact. Part 1. Dynamic Modelling and Stability Analysis, Proc. Instn. Mech. Eng.211 (F) (1997) 11-26.

[8] J. B. Nielsen, Evolution of rail corrugation predicted with a non-linear wear model, Journal of Sound and Vibration 227 (1999) 915-933.

[9] P.A. Meehan, W.J.T. Daniel and T. Campey, Wear-type rail corrugation prediction and prevention, Proceedings of the 6th International Conference on Contact Mechanics and Wear of Rail/Wheel Systems(CM2003) in Gothenburg, Sweden, June 10-13, (2003) 445-454

[10] Igeland, "Railhead corrugation growth explained by dynamic interaction between track and bogie wheelsets", Proc Instn Mech Engrs Part F: Journal of Rail and Rapid Transit, 210 (1996) 11-20.